# Magnetohydrodynamic Analysis of High-Density Plasma Hall Thruster Operation

**IEPC-2025-244**

*Presented at the 39th International Electric Propulsion Conference, Imperial College London, London, United Kingdom*
*14-19 September 2025*

Barth N.[*] Komurasaki, K.[†] Satpathy, D.[‡] Lee J.[§] Sekine H.[¶]
*The University of Tokyo, Hongo, Bunkyo-ku, Tokyo, 113-0033, Japan*

Koizumi H.[‖]
*The University of Tokyo, Kashiwa, Chiba, 277-8561, Japan*

**Hall thrusters are widely used for efficient in-space propulsion, but their reliance on xenon presents challenges in terms of cost and availability. Alternative propellants such as argon or krypton exhibit lower propellant utilization efficiency, motivating thruster designs that increase plasma density within the ionization region. This work investigates such a scaling method using an analytical magnetohydrodynamic (MHD) framework to examine the effects of higher plasma density and magnetic field adjustments. Experimental Hall parameters and anomalous diffusion coefficients of existing thruster designs were estimated using the $J \times B$ force, highlighting differences between SPT and TAL configurations. A fluid-based MHD approach was then applied to identify the principal scaling parameters: mass flow density and magnetic flux density. The framework was demonstrated on the reference TAL-type thruster RAIJIN66. Reducing the anode cross-sectional area increased propellant utilization efficiency but also raised the discharge current and thermal load, which were mitigated by increasing the magnetic flux density. Importantly, while thrust remained essentially constant, the electron current was significantly reduced, illustrating the role of the magnetic field in controlling currents and thermal loads in high-density operation. These results highlight the importance of magnetic field adjustment in maintaining efficient thruster operation under high-density conditions and establish a first-order analytical tool for guiding the design of Hall thrusters using alternative propellants, with potential applications to future high-density, ion-magnetized regimes.**

**Keywords: Hall thruster, TAL, Alternative propellant, Argon, High density, MHD, Permanent magnet**

## Nomenclature

| | |
|---|---|
| $A_{r\theta}, A_{zr}$ | Ionization areas in axial and azimuthal direction |
| $\mathbf{B}$, $B$ | Magnetic field (vector, flux density) |
| $D$, $D_{\parallel}$, $D_{\perp}$ | Diffusion coefficient |
| $\mathbf{E}$, $E_z$ | Electric field (vector, axial component) |
| $I_d$ | Discharge current |
| $I_e$ | Electron current |
| $I_b$ | Ion beam current |
| $I_H$ | Hall current |
| $I_{sp}$ | Specific impulse |

[*]Graduate Student, Department of Aeronautics and Astronautics, The University of Tokyo, n.barth@al.t.u-tokyo.ac.jp
[†]Professor, Department of Aeronautics and Astronautics, The University of Tokyo, komurasaki@al.t.u-tokyo.ac.jp
[‡]Graduate Student, Department of Aeronautics and Astronautics, The University of Tokyo, d.satpathy@al.t.u-tokyo.ac.jp
[§]Graduate Student, Department of Aeronautics and Astronautics, The University of Tokyo, l.jiwon@al.t.u-tokyo.ac.jp
[¶]Assistant Professor, Department of Aeronautics and Astronautics, The University of Tokyo, h.sekine@al.t.u-tokyo.ac.jp
[‖]Associate Professor, Department of Advanced Energy, The University of Tokyo, koizumi@al.t.u-tokyo.ac.jp

| | |
|---|---|
| $\mathbf{j}$, $J$, $j_\theta$, $j_z$ | Current density (vector, azimuthal and axial components) |
| $L_a$, $L_i$ | Acceleration length, ionization length |
| $\dot{m}_A$ | Anode mass flow rate |
| $n_e$, $n_i$, $n_n$ | Electron, ion, and neutral density |
| $P_D$, $P_e$ | Discharge and electron power |
| $\nabla p$ | Pressure gradient term |
| $r_{ge}$, $r_{gi}$ | Electron and ion Larmor radii |
| $r_{\mathbf{in}}$, $r_{\mathbf{out}}$ | Inner and outer channel radii |
| $T$ | Thrust |
| $T_e$ | Electron temperature |
| $\mathbf{v}$, $v_{th}$, $v_i$ | Plasma velocity (bulk, thermal, ion) |
| $v_n$, $v_{nz}$ | Neutral velocity (total, axial) |
| $V_D$ | Discharge voltage |
| $V_{\mathbf{ionization}}$ | Ionization volume $A_{zr}l_\theta$ |
| $\alpha$ | Anomalous diffusion coefficient |
| $\beta$ | Electron Hall parameter |
| $\eta_u$ | Propellant utilization efficiency |
| $\eta$, $\eta_\parallel$, $\eta_\perp$ | Plasma resistivity |
| $\lambda_i$ | Ionization mean free path |
| $\mu$, $\mu_\parallel$, $\mu_\perp$ | Electron mobility |
| $\nu_e$ | Effective electron collision frequency |
| $\nu_{ei}$, $\nu_{en}$, $\nu_a$ | Electron−ion, electron−neutral, and anomalous collision frequency |
| $\omega_{ce}$ | Electron cyclotron frequency |
| $\sigma$, $\sigma_\parallel$, $\sigma_\perp$ | Plasma conductivity |

# I. Introduction

Humanity has made great strides in space exploration over the past 60 years, with satellites playing an important role. Electric propulsion systems, with their high efficiency and low fuel consumption, have become increasingly attractive for long-duration missions. Recent developments by companies such as SpaceX, Boeing and Blue Origin have accelerated the shift towards electric propulsion. Hall-effect thrusters use electric and magnetic fields to ionize and accelerate a propellant, typically xenon, to generate thrust. Figure 1 shows a schematic of a Thruster with Anode Layer (TAL), where propellant enters from the left and collides with electrons supplied by the cathode. These electrons, influenced by the radial magnetic field $B$, gyrate azimuthally along the channel. The propellant atoms (neutrals) are ionized through collisions with the electrons and are then accelerated by an applied axial electric field $E$, generating thrust. In TAL-type Hall thrusters, the anode, which supplies the discharge power, is extended along the channel, and a metallic guard ring is used to protect the magnetic yoke from direct ion bombardment.

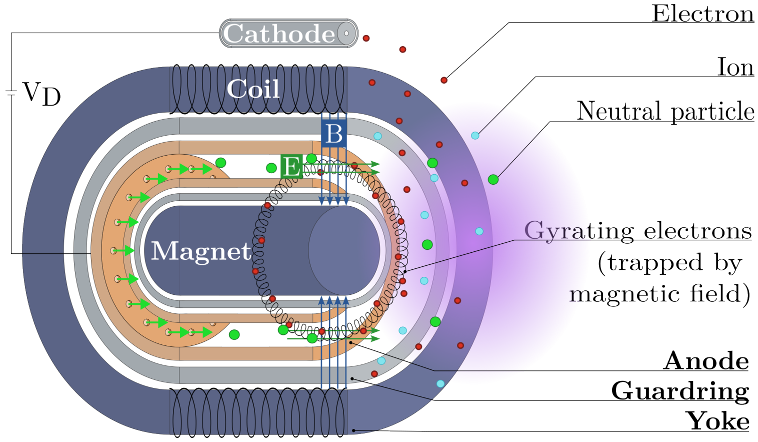


Figure 1: Schematic of a Hall thruster illustrating its basic principles. The figure shows key components such as the anode, guard ring, magnet and coils, and the yoke. Additionally, the directions of the electric and magnetic fields are shown, alongside the behavior of the particles involved in the process, including neutral particles, gyrating electrons, and ions that generate the plasma.

Hall thrusters have been used since the early days of space exploration and are valued for their high specific impulse and long-term operational efficiency. Xenon is considered the optimal propellant due to its high ionic mass and low ionization energy. However, its high cost and limited availability have led to ongoing research into alternative propellants, although no fully viable replacement has yet been identified.[1] While alternative propellants, such as argon and krypton, show promise, they have lower propellant utilization efficiency due to their lower ionic mass and reduced ionization energy. Propellant ionization efficiency $\eta_\mathrm{u}$ is given by Eq. 1:

$$\eta_{\mathrm{u}} = 1 - \exp\left(-\frac{L_{\mathrm{i}}}{\lambda_{\mathrm{i}}}\right) = 1 - \exp\left(-\frac{L_{\mathrm{i}} n_{\mathrm{e}} \langle \sigma_{\mathrm{i}} v_{\mathrm{e}} \rangle}{v_{\mathrm{nz}}}\right) \tag{1}$$

Here $L_{\mathrm{i}}$ represents the ionization region length, $\lambda_{\mathrm{i}}$ the ionization mean free path, $n_{\mathrm{e}}$ is the electron density, $\langle \sigma_{\mathrm{i}} v_{\mathrm{e}} \rangle$ is the ionization rate coefficient, and $v_{\mathrm{nz}}$ is the neutral axial flow velocity, here $v_{\mathrm{nz}} = 1/4 v_{\mathrm{n}}$ with $v_n$ being the neutral flow velocity. Using krypton or argon as propellants reduces the ionization rate coefficient and the ion mass, leading to the lower ionization rates of these propellants.

Two options for improving propellant utilization efficiency are reducing the axial velocity $v_{nz}$, an approach previously attempted by Satpathy by introducing swirl flow[2] and a corrugated shaped anode design,[3] and increasing the plasma density $n_e$, which is the focus of this research.

Recent studies[4] suggest that Hall thrusters have not yet reached their theoretical thrust density limit. Current models operate at approximately $10\,\mathrm{N/m^2}$, well below the theoretical maximum of $1000\,\mathrm{N/m^2}$. This limit is primarily constrained by thermal and material properties. Increasing plasma density $n_e$ is key to approaching this limit, as it enhances ionization efficiency and therefore thrust. To achieve this, neutral density $n_n$ entering the thruster must be increased.

In line with this, this research focuses on increasing the neutral and plasma densities in Hall thrusters. The proposed scaling method involves reducing the thruster area $A_{r\theta}$ while maintaining a constant mass flow rate $\dot{m}_A$, thereby increasing the mass flow density. This approach is expected to increase the neutral density, which in turn enhances the plasma density and improves propellant utilization efficiency. However, such an increase in density also raises the discharge current $I_d$, and therefore the discharge power $P_d$. This can introduce challenges related to higher thermal loads on the thruster, the capability of the power supply, and potential reductions in overall thruster efficiency at increased power levels.

To ensure efficient operation, limit instabilities, and regulate the discharge current, the Hall parameter $\beta$ is introduced as a measure of the relationship between the axial and azimuthal current densities, $j_z$ and $j_\theta$:

$$\beta = \frac{j_\theta}{j_z}. \tag{2}$$

A higher value of $\beta$ indicates stronger electron magnetization. In the following analysis, $\beta$ is used as an indicator of magnetization and as a means to evaluate the magnetic influence on plasma behavior. Controlling the magnetic flux density $B$ is essential to sustain the Hall parameter.

At higher plasma densities, ion–neutral collisions slow down ions, extend their residence time in the channel, and enable additional ionization. These effects make the electrostatic assumption insufficient, as ions can no longer be treated as immediately accelerated and exhausted. Instead, their behavior resembles that of a fluid, making the magnetohydrodynamic (MHD) framework more suitable for describing Hall thruster operation under such conditions.

The following sections introduce the MHD framework employed in this study, with particular attention to the role of the Hall parameter $\beta$. Based on this framework, a scaling method is presented, followed by a discussion of its implications, expected effects, and potential improvements in thruster performance.

## II. Theoretical Framework

In Equation 1, it was shown that the propellant utilization efficiency depends on the ionization length $L_i$ and the ionization mean free path $\lambda_i$. The ionization length $L_i$ is fixed for a given thruster configuration, determined by the geometry and the distribution of the magnetic flux density. In contrast, the ionization mean free path $\lambda_i$ depends on the electron density, which must be estimated iteratively by assuming a value for $\eta_u$.

$$n_e = \frac{I_b}{e v_i A_{r\theta}} = \frac{\dot{m}}{A_{r\theta}} \frac{\eta_u}{v_i m_i}. \tag{3}$$

Equation 3 indicates that the electron density $n_e$ can also be expressed in terms of the ion beam current $I_b$. In practice, however, $I_b$ is usually not directly known and itself depends on the propellant utilization efficiency $\eta_u$, resulting in a recursive relationship.

Using this relation, the ionization mean free path can be estimated as:

$$\lambda_i = \frac{v_{nz}}{n_e \langle \sigma_i v_e \rangle} = \frac{A_c}{\dot{m}} \cdot \frac{v_{nz} v_i m_i}{\eta_u \langle \sigma_i v_e \rangle}. \tag{4}$$

This leads to the following implicit relation for the propellant utilization efficiency $\eta_u$:

$$\eta_{\mathrm{u}} = 1 - \exp\left(-\frac{L_{\mathrm{i}}}{\lambda_{\mathrm{i}}}\right) = 1 - \exp\left(-\frac{L_{\mathrm{i}} n_{\mathrm{e}} \langle\sigma_{\mathrm{i}} v_{\mathrm{e}}\rangle}{v_{\mathrm{nz}}}\right) = 1 - \exp\left(-\frac{\dot{m}_A}{A_{r\theta}} \frac{L_{\mathrm{i}} \eta_u \langle\sigma_{\mathrm{i}} v_{\mathrm{e}}\rangle}{v_i m_i v_{\mathrm{nz}}}\right). \tag{5}$$

Equation 5 highlights the direct dependence of the propellant utilization efficiency on the mass flow density $\dot{m}_A/A_{r\theta}$. In the present approach, propellant utilization is improved by either increasing $\dot{m}_A$ or decreasing $A_{r\theta}$, while keeping other operational parameters, such as the discharge power, constant. However, operating at higher mass flow densities also increases the plasma density, where ion–neutral collisions become significant. These collisions decelerate the ions, extend their residence time in the channel, and facilitate additional ionization events. As momentum is exchanged between ions and neutrals, the ion population can no longer be treated as a set of freely accelerated particles; instead, their collective behavior begins to resemble that of a fluid.

Under the electrostatic assumption, ions are considered to be immediately accelerated and exhausted from the channel, without significant interaction with neutrals. In this framework, ions are not magnetized, and ion–neutral collisions are effectively neglected. However, with higher neutral densities, these collisions slow down the ions and prevent purely electrostatic acceleration from being a valid description of the dynamics.

For this reason, a magnetohydrodynamic (MHD) framework provides a more appropriate description. Within MHD, the Hall current $j_\theta$ and its coupling to the axial current $j_z$ can be explicitly included. This enables the discussion of electromagnetic forces, in particular the $\mathbf{J} \times \mathbf{B}$ force, and provides a natural role for the Hall parameter $\beta$ as a connection between thrust and discharge current $I_d$. While in electrostatic models thrust and discharge are treated separately, thrust through direct ion acceleration and discharge through diffusion losses, the MHD approach allows both to be analyzed simultaneously.

This perspective is particularly important for future Hall thrusters, where higher plasma densities and stronger magnetic fields make ion–neutral interactions unavoidable. In such regimes, ion motion and electron motion can no longer be considered independent, and electrostatic assumptions lose validity. By adopting the MHD framework, it becomes possible to interpret existing experimental data as well as anticipate performance trends in future high-density thruster designs.

The Hall parameter $\beta$ is a key quantity in Hall thruster analysis because it characterizes the degree of electron magnetization and the relative strength of azimuthal to axial current transport. A higher value of $\beta$ indicates stronger coupling of the electrons to the magnetic field, directly influencing cross-field mobility, discharge current, and ultimately thrust production. By linking current transport to plasma behavior, $\beta$ provides a compact measure that connects the electromagnetic properties of the discharge to overall thruster performance. In the following, $\beta$ will be evaluated using different formulations to examine its behavior.

### A. Estimating the Hall parameter from Thrust

In a typical Hall thruster, thrust is calculated as the reaction force due to electrostatic ion acceleration.

$$T_{\mathrm{electrostatic}} = \dot{m}_i v_i \tag{6}$$

However, thrust $T$ can also be described by the cross product of the Hall current density $j_\theta$ and the magnetic field $B$:

$$T_{\mathrm{MHD}} = \int j_\theta \times B = I_H B l_\theta, \tag{7}$$

where $I_H$ is the Hall current, and $l_\theta$ is the mean length of the azimuthal channel. This MHD-based thrust, also known as the $J \times B$ force, is similar to that used in Magnetohydrodynamic (MPD) thrusters. Unlike electrostatic acceleration, this mechanism does not rely on collisions between ions and neutral particles, and it remains effective even under high flow density conditions.

As introduced in Equation 2, the Hall parameter expresses the ratio of the azimuthal current density $j_\theta$ to the axial current density $j_z$. In the following, $\beta$ will be estimated by relating the Hall current density to the measured thrust.

$$\beta = \frac{j_\theta}{j_z} = \frac{I_H/A_{zr}}{I_e/A_{r\theta}}, \tag{8}$$

where $I_H$ and $I_e$ denote the Hall current and the electron current, respectively. The areas correspond to the cross sections through which the currents flow. The axial current density passes through the thruster cross-sectional area $A_{r\theta}$, while the azimuthal current density is associated with a cut area $A_{zr}$, whose effective length is not uniquely defined. For the present analysis, a simplifying assumption is adopted by taking $A_{zr}$ as the product of the ionization region length $L_i$ and the channel width $w$.

The areas and lengths used in the analysis are shown in Figure 2. To address the difficulty of accurately estimating the ionization length, a further simplification is introduced by assuming $L_i = \frac{1}{2}w$. This approximation is consistent with observations from the RAIJIN66 Hall thruster, where the ionization length has been reported to be comparable to the anode width.[5]

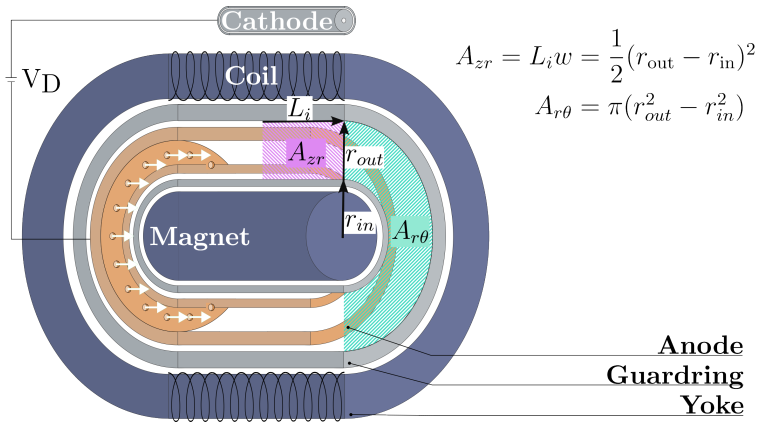


Figure 2: Diagram of a Hall thruster illustrating the areas $A_{zr}$ and $A_{r\theta}$ used in the calculation of the Hall and electron currents, respectively. The area $A_{rz}$ corresponds to the radial-axial plane, while $A_{r\theta}$ corresponds to the radial-tangential plane in the thruster geometry.

In the next step, the electron current $I_e$ must be estimated. This can be approximated as the difference between the discharge current $I_d$ and the ion beam current $I_b$. Neglecting the thrust correction factor $\gamma$, the ion beam current can be expressed as:

$$I_b = n_e e v_i A_{r\theta} = \frac{eT}{m_i v_i}, \tag{9}$$

where $n_e$ is given by $n_e = \dot{m}_A \eta_u / A_{r\theta} v_i m_i$, and $\eta_u = T/\dot{m}_A v_i$. Thus, $I_b$ represents the fraction of the discharge current carried by ions that are accelerated through the channel and contribute directly to thrust production. Consequently, the electron current can be expressed as the difference between the discharge current and the ion beam current:

$$I_e = I_d - I_b. \tag{10}$$

Using these assumptions, the Hall parameter can be estimated by:

$$\beta_{\text{Thrust}} = \frac{I_H}{I_e} \frac{\pi(r_{\text{out}} + r_{\text{in}})}{(r_{\text{out}} - r_{\text{in}})} = \frac{T}{Bl_\theta \left( I_d - \dfrac{Te}{m_i v_i} \right)} \frac{\pi(r_{\text{out}} + r_{\text{in}})}{(r_{\text{out}} - r_{\text{in}})}. \tag{11}$$

The ion velocity $v_i$ can be approximated by assuming that 80% of the discharge voltage $V_d$ contributes to the ion potential drop $\Phi_i$. This formulation shows that the Hall parameter can be estimated using only the thruster geometry, the measured thrust $T$, the magnetic flux density $B$, and the discharge current $I_d$, providing a straightforward way to evaluate this quantity for different existing Hall thrusters. In the following chapter, $\beta_{\text{Thrust}}$ will be estimated for existing Hall thrusters and compared with the diffusion parameters $\beta_{\text{classical}}$ and $\beta_{\text{anomalous}}$, which will be introduced within the following MHD framework.

## B. Magnetohydrodynamic Framework

The MHD model used is derived from the conservation equations of mass, momentum, and energy, treating the plasma as a single conducting fluid. It assumes a Maxwellian velocity distribution, implying sufficient collisionality to sustain local thermodynamic equilibrium.[6]

From the momentum conservation equation, the generalized Ohm' s law can be obtained. This relation will be used in the following analysis to estimate the current densities in the axial ($z$) and azimuthal ($\theta$) directions of the Hall thruster:

$$\mathbf{E} + \mathbf{v} \times \mathbf{B} = \eta \mathbf{j} + \frac{1}{en} (\mathbf{j} \times \mathbf{B} - \nabla p_e) \tag{12}$$

For simplicity, the electric field $\mathbf{E}$ is assumed to exist only in the axial ($z$) direction, while the magnetic field $\mathbf{B}$ is considered to be purely radial ($r$). Under these assumptions, the generalized Ohm' s law can be expressed in vector form as:

$$\begin{pmatrix} j_r \\ j_\theta \\ j_z \end{pmatrix} = \frac{1}{\eta} \begin{pmatrix} 0 \\ 0 \\ E_z \end{pmatrix} + \begin{pmatrix} 0 \\ v_z B_r \\ -v_\theta B_r \end{pmatrix} - \frac{1}{en_e \eta} \left( \begin{pmatrix} 0 \\ j_z B_r \\ -j_\theta B_r \end{pmatrix} - \Delta p_e \right).$$

where $1/\eta = \sigma$ denotes the plasma conductivity, and $1/(en_e\eta) = \mu$ is the plasma mobility.

To estimate the current densities more accurately, we further simplify the model by neglecting the electron velocity in the axial ($z$) direction and the pressure gradient term. Additionally, the electron azimuthal velocity is approximated by the $\mathbf{E} \times \mathbf{B}$ drift velocity ($v_\theta = E_z/B_r$):[7]

$$j_\theta = \sigma v_z B_r - \mu B j_z \approx -\mu B_r j_z = -\beta j_z \tag{13}$$

$$j_z = \frac{\sigma_\parallel E_z}{1 + \beta^2} = \sigma_\perp E_z \tag{14}$$

Equation 28 corresponds to the expression previously used to define the experimental Hall parameter in Equation 2, whereas Equation 14 highlights its dependence on the diffusion regime. These relations show that current transport in magnetized plasmas is inherently anisotropic, a feature that will be examined in more detail when discussing diffusion processes parallel and perpendicular to the magnetic field.

### C. Diffusion Regimes

In a Hall thruster, cross-field electron transport plays a critical role in determining overall efficiency and performance. Ideally, electrons are magnetized and follow classical diffusion behavior, which is driven by collisions with neutrals or ions. However, experiments show that electron transport is much higher than what classical theory predicts. This effect is called Bohm diffusion and is thought to be caused by plasma turbulence, fluctuations, or instabilities, especially in regions with strong electric and magnetic field gradients. In the following, we will mostly consider an anomalous diffusion region that is a mixture between classical and Bohm diffusion.[6]

In both classical and anomalous diffusion, several plasma parameters are used to characterize plasma behavior, including the diffusion coefficient $D$, plasma mobility $\mu$, electrical conductivity $\sigma$, resistivity $\eta$, and electron-neutral collision frequency $\nu_e$.

In a plasma, the transport along the magnetic field lines is usually unaffected by the magnetic field. These plasma parameters parallel to the magnetic field follow standard expressions, as given by Einstein's relation:

$$D = \frac{\mu k_B T}{q}, \tag{15}$$

where $\mu_\parallel = e/(m_e \nu_e)$, $\sigma_\parallel = n_e e \mu_\parallel$, and $\eta_\parallel = 1/\sigma_\parallel$.

In classical diffusion the total electron collision frequency is the sum of the electron–ion and electron–neutral collision frequencies:

$$\nu_e = \nu_{ei} + \nu_{en} = n_i \langle \sigma_{ei} v_{ei} \rangle + n_n \langle \sigma_{en} v_{en} \rangle, \tag{16}$$

where $n_i$ and $n_n$ are the ion and neutral densities, respectively, and $\langle\cdot\rangle$ denotes averaging over the electron velocity distribution function. The cross sections are obtained from LXCAT[8] and are averaged over the velocity using Bolsig+.[9]

In anomalous diffusion, the electron collision frequency is influenced by the anomalous collision frequency $\nu_a$, which represents an effective scattering rate intended to account for turbulence in anomalous diffusion. Consequently, the total electron collision frequency is expressed as follows:

$$\nu_e = \nu_{ei} + \nu_{en} + \nu_a, \tag{17}$$

where $\nu_a = \alpha\omega_c = \alpha eB/m_e$. The bohm diffusion represents a special case of the anomalous diffusion where $\alpha = 1/16$.

When considering the anisotropic behavior of the plasma, we observe that motion perpendicular to the magnetic field is influenced by the Lorentz force. The Hall parameter $\beta$, introduced in equation 2, describes the degree of magnetization and affects the perpendicular plasma parameters. In this context, $\beta$ is often defined as:

$$\beta_{\text{classic}} = \frac{\omega_{ce}}{\nu_e} = \frac{eB}{m_e\nu_e}, \tag{18}$$

where $\omega_{ce}$ is the electron cyclotron frequency, $\nu_e$ is the effective electron collision frequency and $B$ is the magnetic field strength.

Assuming the classical $\beta \gg 1$, the calculation of the diffusion coefficient simplifies as follows:

$$D_\perp = \frac{D_\parallel}{1+\beta^2} \approx \frac{D_\parallel}{\beta^2} = \frac{k_b T_e m_e \nu_e}{e^2 B^2} \tag{19}$$

Similarly, the plasma mobility, conductivity, and resistivity can be expressed as:

$$\mu_{\perp,c} = \frac{\mu_\parallel}{1+\beta^2} \approx \frac{\mu_\parallel}{\beta^2} = \frac{m_e\nu_e}{eB^2}. \tag{20}$$

$$\sigma_{\perp,c} = \frac{\sigma_\parallel}{1+\beta^2} = n_e e \mu_\perp \approx \frac{m_e \nu_e n_e}{B^2}. \tag{21}$$

$$\eta_{\perp,c} = \frac{1}{\sigma_\perp} = \eta_\parallel(1+\beta^2) \approx \frac{B^2}{n_e m_e \nu_e}. \tag{22}$$

The resulting electron collision frequencies, and consequently other perpendicular plasma parameters (except for the resistivity), in classical diffusion are lower than experimental observations. This discrepancy is addressed by introducing empirical parameters in anomalous diffusion:

$$D_{\perp,a} = \alpha\frac{k_B T_e}{eB}, \tag{23}$$

where $\alpha$ is a constant, typically chosen to fit measurements or simulation results. The mobility, conductivity, and resistivity are similarly influenced by the anomalous diffusion coefficient:

$$\mu_{\perp,a} = \frac{eD_{\perp,a}}{k_B T_e} = \frac{\alpha}{B} \tag{24}$$

$$\sigma_{\perp,a} = n_e e \mu_{\perp,a} = \frac{\alpha n_e e}{B} \tag{25}$$

$$\eta_{\perp,a} = \frac{1}{\sigma_{\perp,a}} = \frac{B}{\alpha n_e e} \tag{26}$$

As already mentioned, a common assumption is Bohm diffusion with $\alpha_B = 1/16$. This gives a simple collision frequency of $\nu_e = eB/16m_e$, which corresponds to a constant Hall parameter of $\beta = 16$. However, literature suggests that the Hall parameter varies with different propellants, and the Bohm coefficient of $\alpha = 1/16$ is not always accurate. Smaller values, such as 1/32, 1/44, or even 1/100, have also been reported.

Although anomalous diffusion is often adopted to explain the enhanced cross-field transport in Hall thrusters, both classical and anomalous diffusion are still considered in this analysis. The reason is that, even in the anomalous case, the Hall parameter $\beta$ remains effectively constant for a given operating condition, thereby neglecting possible variations due to collisions. By including both regimes, it becomes possible to compare the idealized behavior predicted by classical transport with the more empirical anomalous description, while also highlighting the limitations that arise when assuming a constant $\beta$.

### D. Estimating the Hall Parameter from Diffusion regimes

In this section, we take a closer look at the two previously introduced current densities in the $\theta$- and $z$-directions, as well as the Hall parameter $\beta$, with respect to the diffusion regime.

#### 1. *Classical Diffusion*

Let us first consider the classical diffusion approach. The current densities introduced in Equations 28 and 14 are used to estimate the resulting currents in the $z$- and $\theta$-directions.

$$j_z = \frac{\sigma_{\parallel} E_z}{1+\beta^2_{\text{classic}}} \approx \frac{\sigma_{\parallel} E_z}{\beta^2_{\text{classic}}} = \frac{n_e e^2 E_z}{m_e \nu_e \beta^2_{\text{classic}}} = \frac{m_e \nu_e n_e E_z}{B^2} \tag{27}$$

showing that the axial current density $j_z$ scales inversely with $\beta^2$, and therefore with $B^2$, in agreement with previous findings.[6]

The resulting current density in the $\theta$-direction is given by:

$$j_\theta = \beta_{\text{classic}} j_z = \frac{n_e e^2 E_z}{m_e \nu_e \beta_{\text{classic}}} = \frac{n_e e E_z}{B}. \tag{28}$$

This result shows that $j_\theta$ scales linearly with $\beta$, indicating that Hall effects dominate cross-field transport at large values of the parameter.

By integrating the electron density in the $z$-direction over the effective ionization area $A_{r\theta}$, we obtain the electron current $I_e$:

$$I_e = \frac{\sigma_{\parallel} E_z A_{r\theta}}{1+\beta^2} \approx \frac{n_e e^2 E_z}{m_e \nu_e \beta^2_{\text{classic}}} A_{r\theta} = \frac{n_e m_e \nu_e E_z}{B^2} A_{r\theta} \tag{29}$$

Similarly, the Hall current $I_\theta$ can be obtained by integrating the azimuthal current density $j_\theta$ over the area:

$$I_H = j_\theta A_{zr} = \frac{n_e e^2 E_z}{m_e \nu_e \beta_{\text{classic}}} A_{zr} = \frac{n_e e E_z}{B} A_{zr}. \tag{30}$$

The Hall current $I_H$ highlights the dependence of the discharge on $n_e$ and $B$.

#### 2. *Anomalous Diffusion*

In the anomalous regime, the current density in the $z$-direction is expressed with $\sigma_\perp = \alpha n_e e/B$ as:

$$j_z = \sigma_\perp E_z = \frac{\alpha n_e e E_z}{B} \approx \frac{n_e e E_z}{\beta_{\text{anomalous}} B}. \tag{31}$$

In the anomalous case, the current density remains finite since $\beta$ is taken as constant, reflecting transport governed by turbulence rather than collisions.

Correspondingly, the current density in the $\theta$-direction is given by:

$$j_\theta = \beta_{\text{anomalous}} j_z = \frac{n_e e E_z}{B}. \tag{32}$$

Then the electron current and the Hall current can be expressed as:

$$I_e = j_z A_{r\theta} = \frac{n_e e E_z}{\beta_{\text{anomalous}} B} A_{r\theta}. \tag{33}$$

$$I_H = j_\theta A_{zr} = \frac{n_e e E_z}{B} A_{zr} \tag{34}$$

The Hall current retains the same form in both classical and anomalous diffusion, in contrast to $I_e$, which changes with the regime.

From equation 33 a definition for anomalous $\beta$ can be given as:

$$\beta_{\text{anomalous}} = \frac{A_{r\theta} n_e e E_z}{I_e B} \tag{35}$$

In Bohm diffusion, this gives $\beta = 16$, whereas in typical Hall thrusters it lies between 16 and the classical value $\beta = eB/m_e\nu_e$.

In order to estimate $\beta_{\text{anomalous}}$ from existing Hall thruster data, additional steps are required beyond the introduction of $\beta_{\text{Thrust}}$. Specifically, the electron density must be inferred from the propellant utilization efficiency using Eq. 3 in combination with experimental measurements. The propellant utilization efficiency itself can be obtained from the measured thrust according to

$$\eta_u = \frac{T}{\dot{m}_A v_i}, \tag{36}$$

where, in this context, the thrust correction factor $\gamma$ is neglected. This approach highlights that the evaluation of $\beta$ relies on experimental observables such as thrust and mass flow rate, thereby allowing $\beta_{\text{Thrust}}$ to be benchmarked against the diffusion parameters $\beta_{\text{classical}}$ and $\beta_{\text{anomalous}}$.

Another important implication concerns the variation of thrust with the Hall parameter $\beta$. At the beginning of this chapter, thrust was introduced both via the electrostatic force (Eq.6) and via the $J \times B$ force (Eq.7). The $\beta$−dependence of the electrostatic expression is not straightforward, because the ion mass flow depends on the propellant utilization efficiency and must be obtained self-consistently with the electron density. By contrast, the MHD expression exhibits an explicit dependence through the Hall current, which has the same form in both diffusion regimes. Consequently, the thrust is independent of the diffusion regime and depends on

$$T = I_H B l_\theta = n_e e E_z A_{zr} l_\theta = n_e e E_z V_{\text{ionization}}. \tag{37}$$

Thus, $T$ depends only on the electron density, the axial electric field, and the ionization volume $V_{\text{ionization}}$.

This formulation in the MHD framework provides a straightforward link between the electron current $I_e$ and the thrust $T$. In contrast to the electrostatic approach, where ion acceleration has to be treated separately and ion−neutral collisions complicate the analysis, the MHD description treats the plasma as a coupled fluid and includes these effects directly. In this way, the thrust can be expressed in terms of discharge quantities such as $I_e$, without the need to isolate individual contributions.

## III. Hall Parameters of State-of-the-Art-Thrusters

In the previous chapter, three methods were introduced to estimate the Hall parameter: directly via the $J \times B$ force (Eq. 11), by the classical approach (Eq. 18), or through the anomalous approach (Eq. 35). It is expected that the Hall parameter for the $J \times B$ force and anomalous diffusion exhibit similar trends, as both ultimately represent the anomalous diffusion observed in experiments.

The literature review revealed that, for some of the thruster data observed in this study, the magnetic flux density was not available. While coil currents are frequently mentioned, no explicit relationship to the magnetic field is provided. In cases where the magnetic field was not explicitly stated, a magnetic flux density of 20 mT was assumed for the calculations. Unfortunately, this implies that the data cannot be considered fully reliable, and the dependence on the magnetic flux density $B$ cannot be demonstrated, as most of the data is estimated with the same magnetic flux density. Instead, the variation of different $\beta$ values will be shown in relation to the range of powers $P_d$, as the discharge conditions and other input parameters, such as mass flow rate, are reflected in the power.

The data utilized in this study is presented in Table 1, which includes the radius, propellant, power level, and magnetic flux density used in the calculation of the three different $\beta$ values.

Figure 3 shows the graphical representation of the calculated classical $\beta_{\text{classic}}$ for different operating conditions. It can be observed that the trend for the classical $\beta_{\text{classic}}$ follows a general increase, with higher $\beta_{\text{classic}}$ values corresponding to higher $P_d$. Additionally, it is evident that the classical $\beta_{\text{classic}}$ is highly dependent on the mass flow rate, as the different linear trends observed are a result of variations in mass flow rate. This dependency is particularly noticeable since the electron collision frequency is strongly influenced by the mass flow rate density, as previously discussed, which leads to the distinct patterns seen in the data. This behavior is specific to classical diffusion; in contrast, in anomalous diffusion, the anomalous collision frequency typically plays a more dominant role.

Both calculations of $\beta_{\text{anomalous}}$ and $\beta_{\text{Thrust}}$ are results of empirically obtained $\beta$ and should include the effect of the anomalous diffusion frequency. Figure 4 shows this comparison for both. It can be seen that ultimately they follow the exact same trend, as originally expected, since both data sets come from empirical values.

Table 1: Calculated mean Hall parameter values from experimental thruster data. Shown are thruster parameters such as power, magnetic flux density, and the three evaluated mean Hall parameters: $\beta_{\text{Thrust}}$, $\beta_{\text{Anomalous}}$, and $\beta_{\text{Classical}}$. Not in all references was the magnetic flux density provided, so in those cases, a magnetic flux density of $B = 20\,\text{mT}$ was assumed.

| Name | Type | $r_{\text{out}}$ | $r_{\text{in}}$ | Prop. | Power | Magnetic flux density | $\beta_{\text{Thrust}}$ | $\beta_{\text{Anomalous}}$ | $\beta_{\text{Classical}}$ | Ref. |
|---|---|---|---|---|---|---|---|---|---|---|
| Units | | mm | mm | | W | mT | - | - | - | |
| D55 | TAL | 36.5 | 18.5 | Xe | 300-2100 | 20 | 344.8 | 107.7 | 244.6 | [10] |
| RAIJIN66 | TAL | 33 | 21 | Ar | 750-1750 | 30 | 42.9 | 13.4 | 197.1 | |
| Tsukuba | TAL | 21.5 | 16.5 | Ar | 240 | 10 | 77.9 | 24.3 | 52.0 | [11] |
| UT-TALI | TAL | 24 | 18 | Ar | 96-120 | 20-60 | 70.3 | 22.0 | 430.5 | [12] |
| KLIMT | SPT | 25 | 17 | Xe | 100-500 | 20 | 318.2 | 99.4 | 389.0 | [13] |
| KLIMT | SPT | 25 | 17 | Kr | 50-400 | 20 | 235.6 | 73.6 | 347.1 | [13] |
| SPT100 | SPT | 50 | 25 | Xe | 500-2100 | 20 | 231.9 | 72.5 | 375.0 | [14–16] |
| SPT100 | SPT | 50 | 25 | Kr | 900-3950 | 20 | 257.4 | 80.4 | 428.1 | [16,17] |
| UT-ThrusterI | SPT | 22 | 15 | Xe | 123-332 | 5-20 | 93.5 | 29.2 | 275.6 | [18] |
| UT-ThrusterI | SPT | 22 | 15 | Ar | 90-616 | 5-20 | 55.8 | 17.4 | 273.6 | [18] |
| UT-ThrusterII | SPT | 24 | 18 | Xe | 130-465 | 100 | 118.7 | 37.1 | 79.7 | [18] |

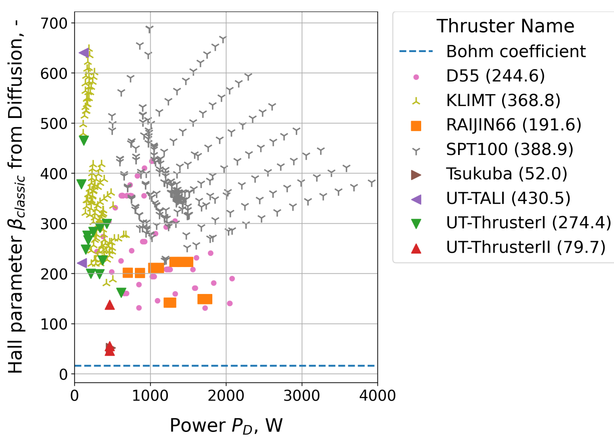


Figure 3: Hall parameter estimated classical diffusion over power, with a horizontal line at $\beta = 16$ indicating the Bohm coefficient. The legend contains the mean Hall parameter for each thruster type.

It can be observed that the values for $\beta_{\text{anomalous}}$ have the lowest numbers, being around 3.2 times lower than the $\beta_{\text{Thrust}}$. In the table and in comparison to the $\beta_{\text{classic}}$, it can be observed that for some of the thruster data, the $\beta_{\text{Thrust}}$ even exceeds the $\beta_{\text{classical}}$, which should be the upper limit for the Hall parameter, as it already considers electron-neutral and electron-ion collisions. This leads to the question of why the $\beta_{\text{Thrust}}$ has higher values for some thrusters. A possible explanation is that the ionization volume for the calculation of the Thrust $\beta$ is underestimated, which leads to the following difference by a factor of 3.2. On the other hand, the Hall parameters calculated by $I_e$ also show some lower Hall parameters than the Bohm coefficient of 16, which is also an unlikely event. One explanation for this could be that some experimental data far from the nominal operating conditions was used, increasing the anomalous collision frequency and leading to a very low Hall parameter. On the other hand, some effects are neglected in this study as well, and some of the assumptions made previously could be questioned.

The experimentally estimated Hall parameters follow the same trend, though the values differ by a linear scaling factor. The true experimental $\beta$ is likely closer to the $\beta_{\text{anomalous}}$, which is derived from the diffusion

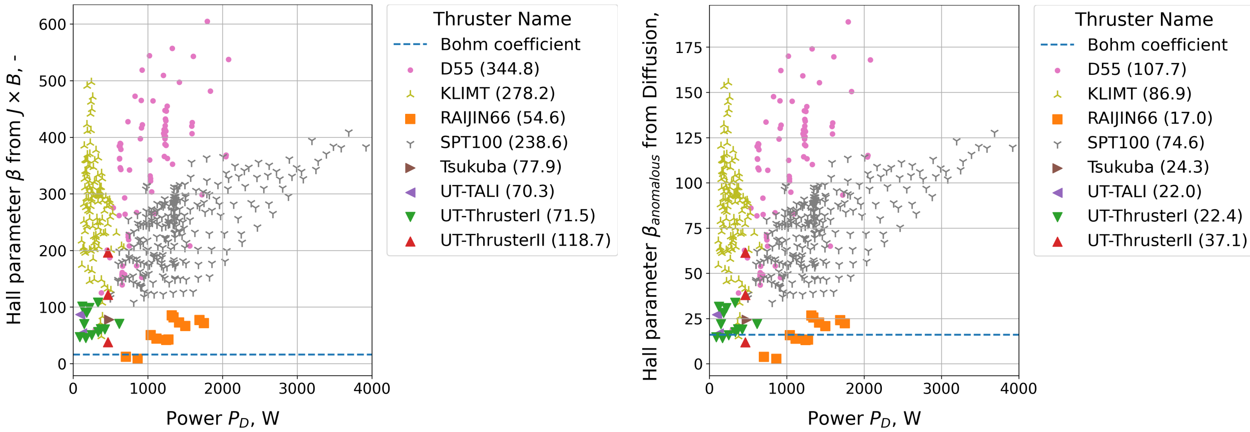


Figure 4: (a) Hall parameter estimated by $J \times B$ force $\beta$ over power and (b) Hall parameter estimated by anomalous diffusion force $\beta$ over power, with a horizontal line at $\beta = 16$ indicating the Bohm coefficient. The legend contains the mean Hall parameter for each thruster type.

theory and the electron current $I_e$.

In conclusion, the Hall parameter is critical for understanding how Hall Effect Thrusters behave, especially in high-density plasma conditions. As plasma density increases, the interaction between axial and azimuthal currents becomes more important, making the traditional electrostatic assumptions no longer sufficient. Ion-neutral collisions start to have a noticeable impact on ion velocity, slowing the ions down and causing them to stay in the channel longer, which leads to increased ionization. The MHD framework is the best approach for understanding these effects, as it accounts for the coupled behavior of ions and electrons in such environments.

From our analysis, it's clear that $\beta$ is key to understanding thruster scaling, particularly when moving from classical to anomalous diffusion regimes. By controlling the magnetic field, we can manage $\beta$ to improve ionization efficiency while keeping thermal loads in check. This is why it' s essential to consider $\beta$ experimentally before scaling a thruster. The relationship between $\beta$ and plasma dynamics directly impacts thruster performance, and as we scale, we' ll need to adjust magnetic fields to keep $\beta$ at optimal levels for efficient operation.

In short, the Hall parameter gives us the necessary insights to scale Hall thrusters properly, and MHD analysis provides the right framework to predict how these thrusters will behave in high-density, high-magnetic-field conditions. Understanding this interaction will be key to designing efficient and stable thrusters for future missions.

## IV. Hall Thruster Scaling

In the previous chapters, we introduced the MHD framework to better understand the effects of high-density operation, incorporating collisions between heavy particles and the implications of slower, slightly ionized, or rotating ions by adopting a fluid approach. We also discussed the importance of the Hall parameter $\beta$, which links thrust and electron current, providing valuable insights into thruster behavior at varying densities. In the following, we will first review existing scaling methods, then present the scaling approach based on the MHD framework, and finally, we will show the results of scaling the RAIJIN66 thruster to a smaller area. This reduction in area increases the mass flow density, thereby enhancing propellant utilization efficiency.

### A. State-of-the-Art Scaling Methods

Over the past several years, numerous scaling methods have been proposed to reduce oscillations and maintain similar plasma parameters in Hall thrusters. Most of these methods are based on, or benchmarked against, the work of Morozov,[19] who identified the ratio between the ionization mean free path $\lambda_i$ and the channel width $w$ as a key scaling parameter. The Morozov-Melikov similarity criterion states that the ratio $\lambda_i/w$ must remain constant to ensure similar plasma behavior across different thruster configurations. He introduced the parameter

$$\frac{\dot{m}}{\pi D}, \tag{38}$$

where $\dot{m}$ is the anode mass flow rate and $D$ the mean channel diameter. This ratio was found to be a significant factor in scaling and was later quantified in[20] for xenon operation, with a recommended lower limit of $\geq 2 \cdot 10^{-2}$ mg/(s · mm).

Since the early development of the Morozov-Melikov similarity criterion, scaling methods for Hall thrusters have been explored worldwide. Among these international efforts, significant advancements were made in Russia by Shagayda,[21,22] who introduced two additional scaling parameters, $K_B$ and $K_M$. Among their findings, it was shown that for a constant discharge voltage $V_d$, the magnetic field strength must be inversely proportional to the channel height. This forms one of the core assumptions of photographic scaling, a method that achieves similar electron energy distribution functions, magnetic field profiles, discharge channel dimensions, and spatial distributions. This makes photographic scaling well-suited for scaling Hall thrusters across different power and size regimes.

In recent years, the advent of machine learning has introduced data-driven approaches to scaling. Plyashkov[23] employed neural networks trained on a large dataset comprising 1,527 operational points from 40 different thrusters. While this approach enables more flexible modeling, it is limited to the data domain of the underlying database and cannot reliably predict outside that range.

In Europe, Andrenucci and colleagues[24,25] examined how variations in diameter $d$, width $w$, and length $l$ affect performance parameters. Alongside the development of a linear scaling method, researchers also investigated radial and geometric scaling approaches.[26,27] Later, Misuri combined earlier scaling efforts into a formal, comprehensive framework.[28,29]

In the United States, Dannenmayer[30] proposed, that an optimal neutral density exists for ionization. He defined the critical neutral density as $n_n = 1.2 \times 10^{19}$ m$^{-3}$, which is the threshold above which increased electron diffusion and heat loads can occur. Conversely, if the neutral density falls below this threshold, the ionization mean free path becomes excessively long, resulting in insufficient ionization. Like other approaches, this method is empirical and based on a database of 33 mostly SPT-type Hall thrusters.

In Japan, Fujita[31] conducted research on the scaling behavior of TAL-type Hall thrusters. He used empirical observations to support the proposed models.

Recently, Lafleur[32] proposed a set of Hall thruster scaling parameters derived from a mathematical model based on new dimensionless quantities $\alpha$, $\beta$, and $\gamma$. These parameters were designed to accommodate different propellants, including xenon, krypton, and argon. The resulting scaling laws were shown to be consistent with those previously reported in the literature.

In addition to conventional scaling approaches, several efforts have specifically targeted increasing plasma density as a means to enhance ionization efficiency. Hofer[33] was one of the first to attempt to increase plasma density. He investigated a two-stage Hall thruster configuration that decouples the ionization and acceleration regions, thereby enabling higher plasma densities.

Another significant development for the increase in plasma density is the Narrow Channel Hall Thruster (NCHT) concept, introduced by Kronhaus.[34–37] Designed for low-voltage, low-mass-flow-rate operation, the NCHT achieves high plasma densities through substantial miniaturization of the discharge channel, with diameter reductions of up to factors of 1:30 and 1:90. This approach enables compact thruster designs while maintaining efficient performance.

A significant recent advancement in high-density Hall thruster development is the H10 thruster.[38] The H10's high-density operation is achieved through optimized channel geometry, advanced thermal management, and magnetic field optitmization. The H10 shows that traditional scaling laws may not apply at these operating levels and highlights the need for updated models that account for such extreme plasma conditions.

All mentioned scaling methods assume that the mass flow rate scales proportionally with the Hall thruster diameter to maintain the condition of collisionless electrostatic acceleration. We suggest that this assumption may break down if the mass flow rate is increased or the diameter is reduced, while keeping the mass flow rate constant. In such cases, a magnetohydrodynamic approach may be necessary to account for the influence of the magnetic field, which is one scope of this research.

It should be noted that the scaling laws discussed here represent only a small part of the extensive research on scaling of Hall thrusters. The literature proposes numerous other approaches and methodologies, each of which contributes valuable insights to different aspects of thruster design and performance. While this review highlights several examples, it does not cover all existing scaling models. The omission of other relevant work is unintentional.

## B. MHD Dependent Hall Thruster Scaling

Previously in this paper, we showed that increasing the mass flow density, $\dot{m}A/Ar\theta$, improves propellant utilization efficiency, while the magnetic flux density $B$ can be adjusted to limit the rise in currents and thermal loads. In this chapter, we analyze how the different diffusion parameters and the resulting thrust theoretically depend on these three key quantities. It should be noted that, due to the recursive nature of the model, where the electron density $n_e$ and propellant utilization efficiency $\eta_u$ are interdependent, the actual effects are more complex than the simple dependencies shown here. The full solutions incorporating these recursive effects will be presented later in the paper.

For now, let us analyze the previously introduced Hall parameter. In the classical regime, $\beta$ is inherently related to $1/\nu_e$, where $\nu_e = \nu_{ei} + \nu_{en}$. In contrast, for Bohm or anomalous diffusion, the Hall parameter depends on $\nu_\alpha = \alpha eB/m_e$, where $\alpha = 1/16$ for Bohm diffusion. As discussed earlier, this means that in the anomalous or Bohm regime, $\beta$ is approximately constant. Small dependencies on $\nu_{ei} + \nu_{en}$ remain, but they are neglected here for simplicity.

In the classical regime, it can be seen that the Hall parameter is inversely proportional to the mass flow density, $\dot{m}A/Ar\theta$:

$$\beta_{\text{classic}} \propto \frac{BA_{r\theta}}{\dot{m}_A}. \tag{39}$$

This expression highlights the role of the magnetic field as the main parameter for regulating the Hall parameter.

The effects on the diffusion parameters, such as $\nu$, $D$, $\mu$, $\sigma$, and $\eta$, are summarized in Table 2 for both classical and anomalous diffusion, showing their dependence on $\dot{m}A$, $Ar\theta$, and $B$.

Table 2: Plasma coefficients for classical and anomalous diffusion.[6,7] The table highlights the dependence on three key scaling parameters: mass flow rate $\dot{m}_A$, ionization area $A_{r\theta}$, and magnetic flux density $B$.

| Parallel to $B$ | Perpendicular to $B$ | |
|---|---|---|
| | Classical Diffusion | Anomalous Diffusion |
| $\nu_e = \nu_{\text{ei}} + \nu_{\text{en}} = n_i\langle\sigma_{ei}v_{th}\rangle + n_n\langle\sigma_{en}v_{th}\rangle$ $\propto \dot{m}_A/A_{r\theta}$ | | $\nu_{\text{Bohm}} = \alpha_B\omega_c = \frac{1}{16}\frac{eB}{m_e}$ $\propto B$ |
| $D_\parallel = \frac{k_bT_e}{m_e\nu_e}$ $\propto A_{r\theta}/\dot{m}_A$ | $D_{\perp,c} = \frac{D_\parallel}{1+\beta^2} \approx \frac{k_bT_em_e\nu_e}{e^2B^2}$ $\propto \dot{m}_A/A_{r\theta}B^2$ | $D_{\perp,B} = \alpha\frac{k_bT_e}{eB}$ $\propto 1/B$ |
| $\mu_\parallel = \frac{e}{m_e\nu_e}$ $\propto A_{r\theta}/\dot{m}_A$ | $\mu_{\perp,c} = \frac{\mu_\parallel}{1+\beta^2} \approx \frac{m_e\nu_e}{eB^2}$ $\propto \dot{m}_A/A_{r\theta}B^2$ | $\mu_{\perp,B} = \frac{eD_B}{kT} = \frac{\alpha}{B}$ $\propto 1/B$ |
| $\sigma_\parallel = n_ee\mu_\parallel = \frac{n_ee^2}{m_e\nu_e}$ $\propto 1$ | $\sigma_{\perp,c} = \frac{\sigma_\parallel}{1+\beta^2} \approx \frac{m_e\nu_en_e}{B^2}$ $\propto \dot{m}_A^2/A_{r\theta}^2B^2$ | $\sigma_{\perp,B} = n_ee\mu_{\perp,B} = \frac{\alpha n_ee}{B}$ $\propto \dot{m}_A/A_{r\theta}B$ |
| $\eta_\parallel = \frac{1}{\sigma_\parallel} = \frac{m_e\nu_e}{n_ee^2}$ $\propto 1$ | $\eta_{\perp,c} = \frac{1}{\sigma_{\perp,c}} \approx \frac{B^2}{m_e\nu_en_e}$ $\propto A_{r\theta}^2B^2/\dot{m}_A^2$ | $\eta_{\perp,B} = \frac{1}{\sigma_{\perp,B}} = \frac{16B}{n_ee}$ $\propto A_{r\theta}B/\dot{m}_A$ |

Similarly, the dependency of the electron and Hall currents in both classical and anomalous diffusion can be shown. In the classical diffusion regime, we obtain

$$
\begin{aligned}
I_e &\propto \frac{\dot{m}_A^2}{Ar\theta B^2} E_z = \frac{A_{r\theta}}{\beta^2} E_z \\
I_H &\propto \frac{\dot{m}_A}{B} \frac{A_{zr}}{A_{r\theta}} E_z = \frac{A_{zr}}{\beta} E_z,
\end{aligned}
\tag{40}
$$

showing that $I_e$ decreases with $\beta^2$ and $I_H$ decreases linearly with $\beta$. The axial electric field $E_z$ is included in the expressions, as it depends on the discharge voltage and the acceleration length $L_a$, which varies with the ionization area $A_{r\theta}$. For simplicity, we assume $L_a = 2L_i$, so that $L_a = 2(r_{\text{out}} - r_{\text{in}})$.

In the anomalous diffusion regime, the scaling becomes

$$
\begin{aligned}
I_e &\propto \frac{\dot{m}_A}{B} E_z \\
I_H &\propto \frac{\dot{m}_A}{B} \frac{A_{zr}}{A_{r\theta}} E_z.
\end{aligned}
\tag{41}
$$

In the anomalous diffusion regime, both currents scale inversely with $B$ and linearly with $\dot{m}_A$, reflecting the approximate constancy of $\beta$ in this regime.

These relationships highlight the role of the Hall parameter in regulating the current distribution and the coupling between electron motion and thrust generation. By adjusting the magnetic field or the ionization volume $V_{\text{ionization}}$, $\beta$ can be controlled to limit currents and thermal loads while maintaining efficient ionization. Together, these scaling laws provide a theoretical framework to predict how changes in geometry, mass flow, and magnetic field influence currents, $\beta$, and thrust, forming the basis for the thruster scaling approach applied to RAIJIN66 in the following sections.

Until now, the recursive effects of electron density and propellant utilization efficiency have been neglected for simplicity. However, these effects influence the electron collision frequency in both diffusion regimes and must therefore be taken into account. In the following, an analytical model is used to include these dependencies and to calculate the resulting changes in diffusion parameters and currents.

### C. Scaling Setup

This chapter applies the recursive model to scale the RAIJIN66 thruster.[31] The analysis focuses on operation with argon, as xenon already achieves high propellant utilization efficiency and does not require further optimization. In contrast, propellants such as krypton and argon present greater potential for efficiency improvements.

The desired increase in density can be achieved either by increasing the mass flow rate or by reducing the ionization area. Here, the latter approach is chosen, as it provides a straightforward and feasible way to modify the thruster design and does not require changes to the experimental setup, which has limited pumping capability for future validation. As a result, the cross-sectional scaling area, $A_{r\theta}$, is reduced.

As discussed in the previous chapter, the magnetic field is used to counteract the increase in electron current. In a first approach, the anode area is reduced and the magnetic field is gradually increased to compensate for the higher electron current and to limit thermal loads. Other parameters, such as mass flow and power, are kept constant in order to isolate the effects of the increased plasma density.

The geometry and magnetic field of the TAL-reference thruster RAIJIN66 are given in Table 3. The anode exit area is used as the reference for scaling, giving the scaled thruster a value of $254, \text{mm}^2$, one quarter of the RAIJIN66 reference area of $1018, \text{mm}^2$, and reducing the channel area by a factor of 2.67.

Different magnetic field conditions are analyzed, based on the scaling factors of the anode and channel. The magnetic flux densities greater than 200 mT are treated as theoretical scenarios, since no permanent magnet material or design strategy has yet been identified that could realize such a high magnetic flux density. The 200 mT case, on the other hand, can be achieved using a permanent magnet in the design.

The reduction in anode area leads to an increase in propellant utilization efficiency, according to Equation 5, by a factor between 1.0 for xenon and 3.1 for argon for a given operational condition at $V_d = 150\,V$, $I_d = 5\,A$, and mass flow rate $\dot{m}_A = 2.1$ mg/s. For the present work, the proportional improvements in $\eta_u$, $n_n$, $n_e$, and $\lambda_i$ are summarized in Table 4.

In the following, the results of the recursive model are presented for both classical and anomalous diffusion, using the scaled thrusters introduced above under the different magnetic flux densities.

Table 3: Geometric parameters of reference thruster RAIJIN66 and scaled variants

| | Anode | | | Channel | | | Magnetic Flux Density |
|---|---|---|---|---|---|---|---|
| | $r_{\text{in}}$ | $r_{\text{out}}$ | $w$ | $r_{\text{in}}$ | $r_{\text{out}}$ | $w$ | |
| RAIJIN66 (Reference) | 24 mm | 30 mm | 6 mm | 21 mm | 33 mm | 12 mm | 50 mT |
| Scaled – 1 $B/B_{\text{ref}}$ | 12 mm | 15 mm | 3 mm | 9 mm | 18 mm | 9 mm | 50 mT |
| Scaled – 2 $B/B_{\text{ref}}$ | 12 mm | 15 mm | 3 mm | 9 mm | 18 mm | 9 mm | 60–100 mT |
| Scaled – 2.7 $B/B_{\text{ref}}$ | 12 mm | 15 mm | 3 mm | 9 mm | 18 mm | 9 mm | 133 mT |
| Scaled – 4 $B/B_{\text{ref}}$ | 12 mm | 15 mm | 3 mm | 9 mm | 18 mm | 9 mm | 200 mT |
| Scaled – 5.4 $B/B_{\text{ref}}$ | 12 mm | 15 mm | 3 mm | 9 mm | 18 mm | 9 mm | 266 mT |
| Scaled – 8 $B/B_{\text{ref}}$ | 12 mm | 15 mm | 3 mm | 9 mm | 18 mm | 9 mm | 400 mT |

Table 4: Proportional improvement factors for a reduced anode area of 1/4 of RAIJIN66

| Reference Area | Anode exit | Channel exit |
|---|---|---|
| $A_{r\theta}$ | 0.375 | |
| $\eta_u$ | 3.1 | |
| $n_n$ | 2.7 | |
| $n_e$ | 8.3 | |
| $\lambda_i$ | 0.1 | |

### D. Recursive Model Results

Similar to the previous section, the results are presented as scaling factors relative to the reference thruster RAIJIN66. Figure 5 shows the scaling of diffusion-related parameters: electron collision frequency $\nu_e$, diffusion coefficient $D$, plasma mobility $\mu$, plasma conductivity $\sigma$, and plasma resistivity $\eta$ over the change in magnetic flux denisty.

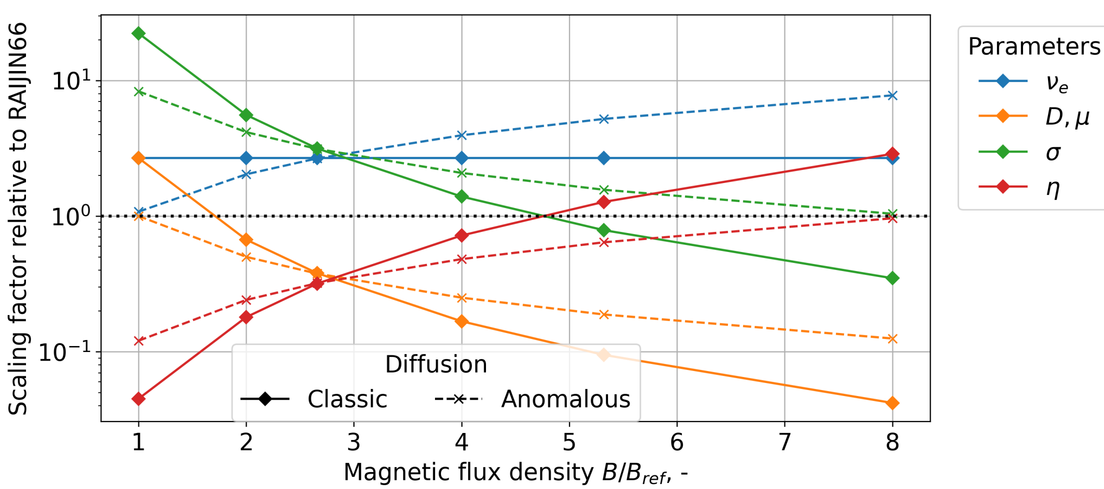


Figure 5: Scaling factors of diffusion-related parameters: electron collision frequency $\nu_e$, diffusion coefficient $D$, plasma mobility $\mu$, plasma conductivity $\sigma$, and plasma resistivity $\eta$, for different magnetic flux densities.

Classical and anomalous diffusion are distinguished by different line styles in the figure, while the black dotted line indicates the baseline at a scaling factor of one, corresponding to the reference thruster RAIJIN66.

As predicted by the proportionalities in Table 2, the results confirm that a stronger magnetic field, at constant plasma density, leads to an increase in the electron collision frequency under anomalous diffusion, since the scaling is proportional to $B$. In contrast, the classical diffusion case shows no dependence on the magnetic field. The diffusion coefficient $D$ and the plasma mobility $\mu$ follow the expected behavior as well: both decrease approximately with $1/B$, starting from values of $1/A_{r\theta}$ and 1, respectively, at low magnetic field. These trends are consistent with the predictions and are reproduced by the recursive model. Similarly, the expected trends for $\sigma$ and $\eta$ are confirmed, following the predicted linear and quadratic dependencies, respectively.

The trends for the diffusion cases do not follow the exact scaling factors, since the classical diffusion model in particular is additionally influenced by the recursively determined electron density. Nevertheless, the fundamental dependencies were already evident from the proportionalities summarized in Table 2.

Similarly Figure 6 shows the scaling of Hall parameter $\beta$, electron current $I_e$, Hall current $I_H$, and thrust estimated by $J \times B$ force $T$.

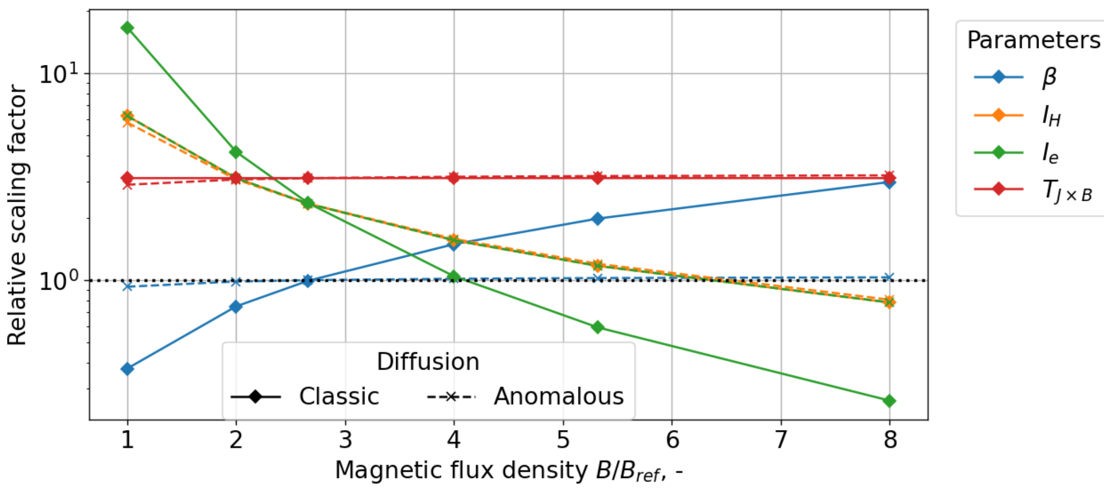


Figure 6: Scaling factors of Hall parameter $\beta$, electron current $I_e$, Hall current $I_H$, and thrust estimated by $J \times B$ force $T$, for different magnetic flux densities. The thrust remains constant with magnetic field, while $I_e$ decreases strongly, showing magnetic control reduces thermal loads without reducing thrust.

On the other hand, the electron current and Hall current do not exactly follow the predicted trends. At the geometric scaling factor of 2.67, both currents are still increased by a factor of 2.3. While the general dependencies of $1/\beta^2$ and $1/\beta$ for the electron and Hall currents, respectively, are still observed, they fail to fully represent the behavior over the magnetic flux density $B$. This indicates that the Hall parameter must be increased further to reduce the heat loads. In this study, an optimal factor of 4 is identified, almost double the geometric scaling factor of 2.67. This deviation is expected to result from the increased collisions caused by the large rise in density in the recursive model.

Another observation that can be made is that the thrust remains essentially unchanged by the change in magnetic flux density. Even though the thrust is calculated using Equation 7, and directly enters the calculation, it does not increase with $B$. This is because the Hall current $I_H$ decreases approximately linearly with the magnetic flux density, and this reduction is exactly compensated by the corresponding increase in $B$, leaving the thrust independent of the magnetic field. In other words, while it is commonly assumed that increasing $\beta$ with $B$ might affect thrust, the actual effect is that the thrust remains constant: the decrease in $I_H$ is canceled out by the higher $B$. The primary benefit of increasing the magnetic flux density is therefore not to increase thrust, but to reduce the electron current $I_e$ and, consequently, the associated heat loads. This leads to an improved situation, where the thruster operates at the same thrust but with lower currents, making the design more efficient and thermally manageable. In the future, this analysis can be extended to high-density thrusters, where ion magnetization could become significant and further influence both the thrust and current distribution.

## E. Limitations of the Model

The analytical MHD model relies on several simplifying assumptions that are necessary to establish a universal scaling framework for Hall thrusters. While these assumptions limit the model's absolute accuracy, they allow it to capture the main scaling tendencies and provide insight into the underlying physics.

A first assumption is that the ionization length is dependent on the channel width, $L_i = 0.5\,w$, which naturally decreases as the thruster is scaled down. In practice, this quantity is highly dependent on thruster design and can vary significantly depending on whether magnetic shielding is employed. For instance, in the case of RAIJIN66, the ionization length is measured to be 5.6 mm without magnetic shielding and 2.1 mm with magnetic shielding, for a channel width of 6,mm.[5] In this work, the variation of $L_i$ with $w$ is introduced to capture the reduction in ionization length for smaller thrusters and to estimate its influence on the propellant utilization efficiency, which is strongly dependent on $L_i$.

Another simplification concerns the magnetic field, which is treated as uniform by considering only the peak magnetic field strength at the thruster exit. Although this is a common assumption in scaling studies, in reality the field follows a Gaussian-like distribution that decreases away from the peak. Since the dominant contribution to electron dynamics occurs near the maximum, this simplification is expected to introduce only minor deviations in the predicted trends.

Furthermore, the model treats classical and Bohm/anomalous diffusion with simplified assumptions, such as a constant Bohm coefficient $\alpha = 1/16$, and does not explicitly account for turbulence or other non-ideal plasma effects.

Thermal effects, wall interactions, and plasma inhomogeneities are not included in the model. As a result, the predictions reflect scaling trends rather than exact quantitative performance, particularly for electron currents, heat loads, or propellant utilization under extreme operating conditions.

Overall, the model represents a zero-dimensional scaling approach that incorporates MHD effects. While it cannot perfectly reproduce experimental data, it provides valuable insight into the trends of Hall thruster parameters and serves as a robust first-order analytical framework for exploring scaling strategies.

## V. Conclusion

Hall thrusters are promising candidates for efficient in-space propulsion, but their reliance on xenon comes with cost and availability challenges. Alternative propellants such as argon or krypton generally have lower propellant utilization efficiency, which motivates designs that increase plasma density in the ionization region. In this work, an analytical magnetohydrodynamic (MHD) approach was used to study how increased plasma density and adjustments in the magnetic field affect thruster performance.

The MHD framework is particularly important in this context because it captures the effects of heavy-particle collisions and the coupled dynamics of electrons and ions, which become increasingly significant at higher plasma densities. By deriving the Hall parameter from the $J \times B$ force using experimental data, the model enables a consistent assessment of thruster behavior under both classical and anomalous diffusion regimes. This highlights the validity of MHD in describing the interactions between electron current, Hall current, and plasma density—interactions that cannot be fully captured by purely electrostatic models, especially under the consideration of high-density operation where ion dynamics and collisions play a dominant role.

From the analysis, the mass flow rate $\dot{m}_A$, the ionization area $A_{r\theta}$ (i.e., the mass flow density), and the magnetic flux density $B$ were identified as the principal scaling parameters. Applying the scaling method to the reference thruster RAIJIN66 showed that reducing the anode cross-sectional area increases propellant utilization efficiency, but also raises the discharge current and thermal load. Increasing the magnetic flux density by a factor of four reduces the electron current $I_e$ by roughly one order of magnitude while leaving the thrust essentially unchanged. This confirms that, in the current regime with unmagnetized ions, thrust is largely independent of the magnetic field: decreases in Hall current are exactly compensated by the higher magnetic flux, so the magnetic field primarily serves to control currents and thermal loads rather than to increase thrust.

The analysis relied on several simplifying assumptions, including the scaling of the ionization length with the channel width and the uniform treatment of the magnetic field. While these assumptions limit the predictive accuracy of the model, they allow the main scaling trends to be identified and demonstrate the usefulness of the MHD framework in capturing the interplay between plasma density, magnetic field, and overall thruster performance.

In summary, the MHD-based scaling method provides a first-order analytical tool for examining Hall thruster operation in the high-density regime. It demonstrates the potential of compact, high-density thruster designs to improve propellant utilization efficiency while maintaining stable thrust and reduced thermal loads. Importantly, while ions are unmagnetized in the present study, future high-density thrusters may operate in regimes where ion magnetization becomes significant. In such cases, neglecting MHD effects is no longer valid, and the framework presented here will be essential for accurately predicting performance and guiding the design of thrusters optimized for alternative propellants, high plasma density, and more extreme operational conditions.

## Acknowledgments

This work was supported by the Japan Society for the Promotion of Science (JSPS) KAKENHI Grant Number 25K01416. The ESA Conference Student Sponsorship Programme provided financial support for attending the conference.

## References

[1]Tirila, V.-G., Demairé, A., and Ryan, C. N., "Review of alternative propellants in Hall thrusters," *Acta Astronautica*, Vol. 212, 2023, pp. 284–306.

[2]Satpathy, D., Sekine, H., Lee, J., Komurasaki, K., Kawashima, R., and Koizumi, H., "Influence of propellant injection directionality on the performance of an argon Hall thruster," *Journal of Applied Physics*, Vol. 136, No. 23, 2024.

[3]Satpathy, D., Sekine, H., Lee, J., Barth, N., and Komurasaki, K., "Enhancement of neutral particle density by propellant reversal through a sawtooth hollow anode," 39st International Electric Propulsion Conference, 2025.

[4]Simmonds, J., Raitses, Y., and Smolyakov, A., "A theoretical thrust density limit for Hall thrusters," *Journal of Electric Propulsion*, Vol. 2, No. 1, 2023, pp. 12.

[5]Satpathy, D., Sekine, H., Barth, N., Kawashima, R., Komurasaki, K., and Koizumi, H., "Experimental investigation on ionization length required for efficient operation of argon Hall thrusters," *Transactions of the Japan Society for Aeronautical and Space Sciences*, Vol. 68, No. 1, 2025, pp. 12–18.

[6]Francis, F. C., *Introduction to plasma physics and controlled fusion*, Spinger, 2016.

[7]Goebel, D. M., Katz, I., and Mikellides, I. G., *Fundamentals of electric propulsion*, John Wiley & Sons, 2023.

[8]Pitchford, L. C., Alves, L. L., Bartschat, K., Biagi, S. F., Bordage, M.-C., Bray, I., Brion, C. E., Brunger, M. J., Campbell, L., Chachereau, A., et al., "Lxcat: An open-access, web-based platform for data needed for modeling low temperature plasmas," *Plasma Processes and Polymers*, Vol. 14, No. 1-2, 2017, pp. 1600098.

[9]Hagelaar, G. and Pitchford, L. C., "Solving the Boltzmann equation to obtain electron transport coefficients and rate coefficients for fluid models," *Plasma sources science and technology*, Vol. 14, No. 4, 2005, pp. 722.

[10]Sankovic, J. M., Haag, T. W., and Manzella, D. H., "Operating Characteristics of the Russian D-55 Thruster with Anode Layer," Tech. Rep. NASA-TM-106610, NASA Lewis Research Center, Cleveland, OH, United States, June 1994, Presented at the Joint Propulsion Conference, Indianapolis, IN, June 27–30, 1994.

[11]Yamasaki, J., Yokota, S., and Shimamura, K., "Performance enhancement of an argon-based propellant in a Hall thruster," *Vacuum*, Vol. 167, 2019, pp. 520–523.

[12]Komurasaki, K., Mikami, K., and Kusamoto, D., "Channel length and thruster performance of Hall thrusters," *32nd Joint Propulsion Conference and Exhibit*, 1996, p. 3194.

[13]Kurzyna, J., Jakubczak, M., Szelecka, A., and Dannenmayer, K., "Performance tests of IPPLM's krypton Hall thruster," *Laser and particle beams*, Vol. 36, No. 1, 2018, pp. 105–114.

[14]Brophy, J. R., "Stationary plasma thruster evaluation in Russia," Tech. rep., 1992.

[15]Sankovic, J. M., Hamley, J. A., and Haag, T. W., "Performance evaluation of the Russian SPT-100 thruster at NASA LeRC," *IEPC Conference*, No. IEPC-93-094, 1994.

[16]Hargus, M. R. N. J., Delgado William, A., Corey Jorge, J., and Ronald, L., "A Performance Comparison of Xenon and Krypton Propellant on an SPT-100 Hall Thruster (Preprint)," *(No Title)*, 2011.

[17]Misuri, T., Battista, F., Barbieri, C., De Marco, E. A., Andrenucci, M., et al., "High power Hall thruster design options," *Proceedings of the 30th International Electric Propulsion Conference (Florence), IEPC*, 2007, pp. 07–311.

[18]Komurasaki, K. and Arakawa, Y., "Hall Current lon-Thruster Performance," *Journal of Propulsion and Power*, Vol. 8, No. 6, 1992, pp. 1212–1216.

[19]Morozov, A. and Melikov, I., "On similarity of processes in plasma accelerators with closed electron drift in conditions of ionization," *Zhurnal Tekhnicheskoj Fiziki*, Vol. 44, No. 3, 1974, pp. 544–548.

[20]Bugrova, A., Lipatov, A., Morozov, A., and Churbanov, D., "On a similarity criterion for plasma accelerators of the stationary plasma thruster type," *Technical Physics Letters*, Vol. 28, 2002, pp. 821–823.

[21]Shagayda, A. A. and Gorshkov, O. A., "Hall-thruster scaling laws," *Journal of Propulsion and Power*, Vol. 29, No. 2, 2013, pp. 466–474.

[22]Shagayda, A. A., "On scaling of Hall effect thrusters," *IEEE Transactions on Plasma Science*, Vol. 43, No. 1, 2014, pp. 12–28.

[23]Plyashkov, Y. V., Shagayda, A. A., Kravchenko, D. A., Lovtsov, A. S., and Ratnikov, F. D., "On scaling of Hall-effect thrusters using neural nets," *Journal of Propulsion and Power*, Vol. 38, No. 6, 2022, pp. 935–944.

[24]Andrenucci, M., Biagioni, L., Marcuccio, S., and Paganucci, F., "Fundamental scaling laws for electric propulsion concepts," *28th International Electric Propulsion Conference*, 2003, p. 1721.

[25]Andrenucci, M., Battista, F., Piliero, P., et al., “Hall thruster scaling methodology,” *The 29th Int. Electric Prop. Conf., Princeton University, 31 October–4 November 2005*, 2005.

[26]Hargus Jr, W. A., *Investigation of the plasma acceleration mechanism within a coaxial Hall thruster*, Stanford University, 2001.

[27]Ahedo, E. and Gallardo, J., “Low power Hall thrusters: physics, technical limitations and design,” *Micropropulsion Workshop, Lerici, Italy*, 2002.

[28]Misuri, T., Battista, F., Barbieri, C., De Marco, E. A., Andrenucci, M., et al., “High power Hall thruster design options,” *Proceedings of the 30th International Electric Propulsion Conference (Florence), IEPC*, 2007, pp. 07–311.

[29]Misuri, T. and Andrenucci, M., “HET scaling methodology: Improvement and assessment,” *44th AIAA/ASME/SAE/ASEE Joint Propulsion Conference & Exhibit*, 2008, p. 4806.

[30]Dannenmayer, K. and Mazouffre, S., “Elementary scaling laws for sizing up and down Hall effect thrusters: Impact of simplifying assumptions,” *Proceedings of the 31st International Electric Propulsion Conference (Ann Arbor), IEPC*, 2009, pp. 09–077.

[31]Fujita, D., *Scaling Law for Argon Anode Layer Hall Thrusters*, Ph.D. thesis, Master thesis, University of Tokyo, 2014.

[32]Lafleur, T. and Chabert, P., “Similarity parameters and scaling laws for hall thrusters,” *Plasma Sources Science and Technology*, Vol. 34, No. 5, 2025, pp. 055005.

[33]Hofer, R. R., Peterson, P. Y., Gallimore, A. D., and Jankovsky, R. S., “A high specific impulse two-stage Hall thruster with plasma lens focusing,” IEPC-01-036, 27th International Electric Propulsion Conference, Pasadena, CA, 2001.

[34]Kronhaus, I. and Linossier, A., “Experimental characterization of the narrow channel Hall thruster,” *Plasma Sources Science and Technology*, Vol. 27, No. 12, 2018, pp. 124005.

[35]Kronhaus, I. and Hamo, O., “2D particle-in-cell channel simulation of the narrow channel Hall thruster,” *36th International Electric Propulsion Conference, IEPC-2019-642, Vienna, Austria*, 2019, pp. 15–20.

[36]Hamo, O. and Kronhaus, I., “Experimental and numerical characterization of the narrow channel Hall thruster discharge,” *Journal of Applied Physics*, Vol. 130, No. 22, 2021.

[37]Kronhaus, “Geometrical Scaling of the Narrow Channel Hall Thruster,” *IEPC - International Conference of Electric Propulsion*, 2024.

[38]Hofer, R. R., Simmonds, J. B., Goebel, D. M., Steinkraus, J. M., and Payman, A. R., “The H10 high power density hall thruster,” *Journal of Electric Propulsion*, Vol. 4, No. 1, 2025, pp. 1–26.